MEASUREMENT OF MASS DISTRIBUTION PARAMETERS OF ANATOMICAL SEGMENTS

Edward B. Becker

Naval Aerospace Medical Research Laboratory
Pensacola, Florida

October 1973

NAMRL - 1193

MEASUREMENT OF MASS DISTRIBUTION PARAMETERS OF ANATOMICAL SEGMENTS

Edward B. Becker

October 1973

NAVAL AEROSPACE MEDICAL RESEARCH LABORATORY
PENSACOLA FLORIDA

Unclassified

Security Classification

DOCUMENT CONTROL DATA - R & D

(Security classification of title, body of abstract and indexing annotation must be entered when the overall report is classified)

1. ORIGINATING ACTIVITY (Corporate author) Naval Aerospace Medical Research Laboratory Naval Aerospace Medical Institute Naval Aerospace and Regional Medical Center Pensacola, Florida 32512	2a. REPORT SECURITY CLASSIFICATION Unclassified 2b. GROUP

3. REPORT TITLE

MEASUREMENT OF MASS DISTRIBUTION PARAMETERS OF ANATOMICAL SEGMENTS

4. DESCRIPTIVE NOTES *(Type of report and inclusive dates)*

5. AUTHOR(S) *(First name, middle initial, last name)*

Edward B. Becker

6. REPORT DATE	7a. TOTAL NO. OF PAGES	7b. NO. OF REFS
October 1973	34	1

8a. CONTRACT OR GRANT NO	9a. ORIGINATOR'S REPORT NUMBER(S)
ONR N00014-69-A-0248-0001 b. PROJECT NO. M4512.01-5001BE1J c. d.	NAMRL - 1193 9b. OTHER REPORT NO(S) *(Any other numbers that may be assigned this report)*

10. DISTRIBUTION STATEMENT

Approved for public release; distribution unlimited.

11. SUPPLEMENTARY NOTES	12. SPONSORING MILITARY ACTIVITY

13. ABSTRACT

Procedures to determine the center of mass and the moments of inertia in three dimensions of previously defined anatomical segments are presented. As an illustration, these procedures are applied to the human head and head-and-neck. The results of measurements made on six human heads and three head-and-necks are presented and discussed.

DD FORM 1 NOV 68 1473 (PAGE 1)

S/N 0101-807-6801

Unclassified

Security Classification

Unclassified

Security Classification

14 KEY WORDS	LINK A		LINK B		LINK C	
	ROLE	WT	ROLE	WT	ROLE	WT
Biomechanics						
Bioengineering						
Center of Gravity						
Moment of Inertia						
Trifilar Pendulum						
Anatomical Segments						

DD FORM 1 NOV 68 1473 (BACK)

(PAGE 2)

Unclassified

Security Classification

Approved for public release;
distribution unlimited

MEASUREMENT OF MASS DISTRIBUTION PARAMETERS OF ANATOMICAL SEGMENTS

Edward B. Becker

Bureau of Medicine and Surgery
M4312.01-5001BE1J

and

Office of Naval Research
Contract N00014-69-A-0248-0001

Approved by

Ashton Graybiel, M.D.
Assistant for Scientific Programs

Released by

Captain N. W. Allebach MC USN
Officer in Charge

26 October 1973

Naval Aerospace Medical Research Laboratory
Naval Aerospace Medical Institute
Naval Aerospace and Regional Medical Center
Pensacola, Florida 32512

SUMMARY PAGE

THE PROBLEM

In the formulation of lumped parameter models to predict the dynamic response of the human body such rigid body characteristics as constant mass, center of mass, and moments of inertia are ascribed to anatomical segments. The subject of this report is a technique for direct measurement of these quantities.

FINDINGS

The measurement techniques were performed on embalmed specimen human heads and human head and necks. The mass distribution parameters as measured are within five percent of the actual specimen value, but the specimens themselves are changed considerably from the living state as a result of the embalming procedures.

RECOMMENDATIONS

These measurement techniques can be successfully applied to anatomical segments of interest, but care should be taken to keep the specimen segment from deteriorating. The most promising method of preservation at this time is the deep freezing of the anatomical segment as soon as possible in order to stabilize the body fluids within the segment.

720964

Measurement of Mass Distribution Parameters of Anatomical Segments

Edward B. Becker
Naval Aerospace Medical Research Laboratory

Reprinted January 1973 from
Sixteenth Stapp Car Crash Conference, P-45, by
SOCIETY OF AUTOMOTIVE ENGINEERS, INC.,
Two Pennsylvania Plaza, New York, N.Y. 10001

iv

720964

Measurement of Mass Distribution Parameters of Anatomical Segments

Edward B. Becker
Naval Aerospace Medical Research Laboratory

Abstract

Procedures to determine the center of mass and the moments of inertia in three dimensions of previously defined anatomical segments are presented. As an illustration, these procedures are applied to the human head and head-and-neck. The results of measurements made on six human heads and three head-and-necks are presented and discussed.

IN THE FORMULATION of lumped parameter models to predict the dynamic response of the human body, such rigid-body characteristics as constant mass, center of mass, and moments of inertia are ascribed to various anatomical segments. Since most of these segments are notoriously not rigid bodies, the best rigid-body approximation for any particular response could be derived only from an extensive study of that response. Even so, the mass distribution of a particular body segment for the static case (that is, for motions so slight as to cause no deformation of the soft tissues) can serve as an initial estimate of the best rigid-body approximation of this segment for more complex behavior.

The procedures outlined in this paper are discussed with respect to a particular anatomical body, the human head. It is felt that the exhaustive treatment given the problem of applying the subject measurement procedures to the human head and the human head-and-neck will sufficiently illustrate the techniques for application to other anatomical sections.

Any attempt to measure directly the rigid-body characteristics of the head and of the head-and-neck must include a treatment of certain factors, such as:

1. The human head and head-and-neck have no definite physical demarcation.
2. Neither the head nor the head-and-neck is a rigid body.
3. The physical structure of these bodies varies from individual to individual, obscuring the selection of anatomical landmarks with which to locate and align these parameters.

These factors are treated as follows:

1. The physical limits of the head and the head-and-neck are defined by the same anatomical procedures as those used in Ref. 1.
2. Two factors compromise the rigidity of the these bodies. Each is composed of jointed bodies, which can assume a number of positions, and each is composed of large amounts of soft tissue. These bodies are made to approximate rigid bodies by selecting a single configuration (jaw shut and the cervical spine in a rigid but uncontrolled set) and employing measuring procedures that minimize relative motions of the soft tissues.
3. The auditory meatuses and the orbital notches, which define Reade's plane, are used to define a three-dimensional coordinate system (Fig. 1) in which these parameters are then located. In this manner, these mechanical characteristics are fixed in the bony structure of the skull.

The measuring procedures employed require that a further bargain with physical reality be struck before any measurements are made. In order to make these measurements, the head or the head-and-neck must be physically separated from the rest of the body. Therefore, these procedures are performed upon cadaveric material in hopes that a statistical evaluation of the information obtained will relate these mechanical parameters to such measurements as may be made on living subjects.

Since the subjects on which these measurements were made were prepared at Tulane University for measurements of these parameters in two dimensions (that is, the location of the center of mass in the midsagittal plane and the moment of inertia about an axis perpendicular to this plane), this study will be concerned primarily with the procedures and mathematics necessary to obtain the complete center of mass vector and moment of inertia tensor. The anatomical preparation, the ages, and the histories of the subjects are reported in Ref. 1.

These measurement procedures are designed to maximize operational simplicity and redundancy at the expense of computational complexity. In this manner, procedural errors are minimized, while transcription errors may be recognized and eliminated during the data reduction without compromising the results.

The bulk of these procedures involve measurements made on a single piece of equipment, the stereotaxic jig. This jig is composed of a David Kopf Industries Model 1630 stereotaxic unit set into a tetrahedral frame. The frame is designed to facilitate those measurements necessary to obtain the center of mass and the

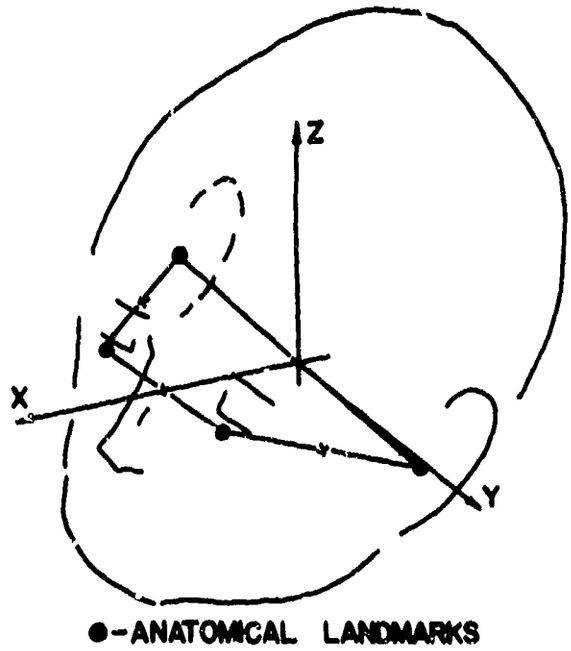

Fig. 1 - Head-referenced coordinates

moment of inertia. The stereotaxic unit is designed to locate and secure the subject within it.

Once obtained, the center of mass and the moment of inertia of the subject-jig combination and the empty jig can be compared to yield the subject center of mass and moment of inertia. Once the subject has been located within the jig, these mechanical parameters can be transformed to anatomically based coordinates.

Procedures Apparatus

The apparatus can be separated into three groups by function: the subject procedure interface, the center of mass equipment, and the moment of inertia equipment.

The subject procedure interface consists of the jig and a DKI 1760 micromanipulator. The jig (Fig. 2) is a specially adapted DKI Model 1630 stereotaxic unit set into a tetrahedral frame. This stereotaxic unit secures the subject by means of two bars inserted into the auditory meatuses, two more bars placed on the inferior orbital ridges over the orbital notches, and a fifth bar placed under the chin.

The tetrahedral frame is specially designed to contain the stereotaxic unit and to facilitate the functions of the two other equipment groups. It is built in the form of a tetrahedron with projections at the vertexes and at the midpoints of each edge.

The micromanipulator is a multijointed arm designed to position probes, electrodes, and the like. It is used as outlined in Appendix D to locate the auditory meatuses and the notch on each of the inferior orbital ridges of a subject secured in the jig. The locations of these four points then yield the precise position and alignment of the subject with respect to the jig. The center of mass equipment consists of a single-arm balance calibrated to 0.02 lb.

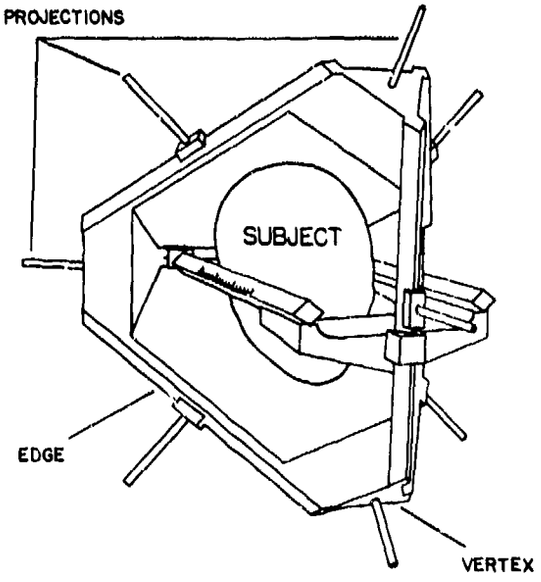

Fig. 2 - Stereotaxic unit and tetrahedral frame

By positioning the jig so that it is supported by three of the edge-midpoint projections and resting one of the three projections on the balance, it is possible to measure the load supported by that projection.

In actual fact, a problem intrudes here. For this particular equipment configuration, there is no stable equilibrium; the balance arm can never be leveled, but will always be at some extreme limit, high or low, of its travel. An explanation of this phenomenon is included in Appendix A. The measurement made is that weight at which the balance pan moves from its highest to its lowest position. This procedure introduces definite errors into the measurements, but these errors negate each other in the data reduction.

There are four different positions in which the jig may be placed so that it is supported by three of the edge-midpoint projections, yielding a total of 12 measurements that can be made. These 12 measurements then yield the three-dimensional position of the c.g. of the jig.

The moment of inertia equipment consists of three wires, whose ends may be looped about three of the jig's projections suspending it in the manner of a trifilar pendulum, and the timing equipment. The timing equipment is composed of a 500 W slide projector, a mirror, a photosensitive trigger, and a countertimer. The projector beam, trimmed by placing a razor in the slide receptacle, reflects from a mirror attached to the jig, and is focused onto the photosensitive trigger. This trigger is placed as near the projector as possible so that while rotational motion of the jig sweeps the beam across the trigger, translational motion produces no discernible beam displacement. This trigger then activates the countertimer, permitting accurate measurement of the rotational period of the jig.

There are four different orientations in which the jig may be suspended by three vertex projections, and six more orientations in which the jig may be suspended by two vertex projections and the edge-midpoint projection between the two unused

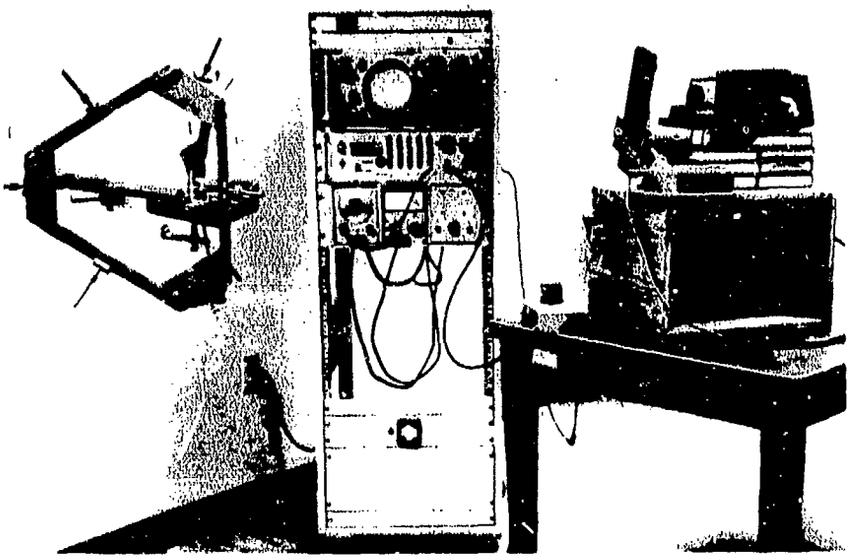

Fig. 3 - Moment of inertia procedures

vertexes, as shown in Fig. 3. The rotational periods of the trifilar pendulums formed by hanging the jig in these 10 different orientations are measured, and these 10 measurements yield the full three-dimensional inertia tensor.

Mathematics

Most of this section is devoted to describing transformations between four separate coordinate systems. The first of these coordinate systems, shown in Fig. 1, is the one fixed in the bony structure of the human skull.

Four anatomical landmarks, the right and left auditory meatuses and the notches on the right and left inferior orbital ridges, locate the head coordinates using the algorithms in Appendix C. The X-Y plane is the plane that passes through the midpoints of the lines connecting the two auditory meatuses, the two orbital notches, the right auditory meatuses and the right orbital notch, and the left auditory meatus to the left orbital notch.

Proof that these four points are coplanar is provided in Appendix B. The first of these midpoints is the origin. This point and the second midpoint locate the X-axis. The Y-axis is parallel to a line through the third and the last of these midpoints. The X-axis is positive in the forward-facing direction, the Y-axis is positive on the left side, and the Z-axis, defined by $\hat{x} \times \hat{y}$, is positive through the top of the skull.

The second of these coordinate systems is located in the jig hardware. This system is chosen for its rough alignment with the coordinate system of a subject secured within it, and is described in terms of the subject. The origin is the vertex behind and to the right of the right ear. The Y-axis is along the edge connecting the origin to the vertex behind and to the left of the left ear. The X-axis is parallel to the line connecting the midpoint of the Y-axis edge to the midpoint of the edge on the opposite side of the tetrahedron. This edge is the only one of the five remaining edges with which the Y-axis edge has no direct contact. This particular edge is also parallel to the Z-axis. Positive directions are head left, up, and facing, respectively.

The remaining two coordinate systems are fixed in the procedures. The $\hat{x} - \hat{y}$ plane in the c.g. procedures is the plane through the points on which the jig's three supporting projections rest. The origin is the point of contact between the projection whose loading is being measured and the balance pan. The $\hat{x}$-axis passes through the origin and is perpendicular to the line through the other two contact points. The $\hat{z}$-axis is positive upward and parallel to the gravity vector.

The $\hat{x} - \hat{y}$ plane in the moment of inertia procedures passes through the loops at the ends of the three wires. The $\hat{z}$-axis is positive upward and parallel to the gravity vector. Taking one of these loops as the origin, the $\hat{y}$-axis is positive through the next loop going clockwise (looking down). The $\hat{x}$-axis is defined by $\hat{y} \times \hat{z}$.

In performing a complete set of measurements, the subject assumes one orientation relative to the jig. The jig assumes 12 orientations to the c.g. procedures and 10 orientations to the moment of inertia procedures, each of these 22 procedural orientations being assumed twice.

The orientation of the head relative to the jig is defined by a cosine matrix and a vector

$$\begin{bmatrix} x \\ y \\ z \end{bmatrix}_{jig} = \begin{bmatrix} t_{11} & t_{12} & t_{13} \\ t_{21} & \cdot & \cdot \\ t_{31} & \cdot & \cdot \end{bmatrix} \begin{bmatrix} x \\ y \\ z \end{bmatrix}_{head} + \begin{bmatrix} b_1 \\ b_2 \\ b_3 \end{bmatrix} \tag{1}$$

The 22 orientations of the jig to the procedures are also defined by cosine matrixes and displacement vectors.

In the c.g. procedures, the theoretical load supported by the projection is

$$W\,\text{theoretical} = W\,\text{total}\left[1 - \frac{X_{\text{c.g.}}}{X_t}\right] \tag{2}$$

where:

$X_{\text{c.g.}}$ = $\bar{x}$ position of jig c.g. in procedural coordinate system
X_t = length of line from projection perpendicular to line connecting other two projections

X_t is the same for all 12 orientations, but $X_{\text{c.g.}}$ is given by

$$X_{\text{c.g. procedures}} = [t_{11n}\, t_{12n}\, t_{13n}]\begin{bmatrix} X_{\text{c.g.}} \\ Y_{\text{c.g.}} \\ Z_{\text{c.g.}} \end{bmatrix}_{\text{jig}} + b_{1n} \tag{3}$$

where:

n = orientation

Combining these two equations gives a relation in the form

$$\frac{W\,\text{theoretical}}{W\,\text{total}} = C_{1n}X_{\text{c.g. jig}} + C_{2n}Y_{\text{c.g. jig}} + C_{3n}Z_{\text{c.g. jig}} + C_{4n} \tag{4}$$

where:

$$C_{1n} = -\frac{t_{11n}}{X_t} \tag{5}$$

$$C_{2n} = -\frac{t_{12n}}{X_t} \tag{6}$$

$$C_{3n} = -\frac{t_{13n}}{X_t} \tag{7}$$

$$C_{4n} = 1 - \frac{b_{1n}}{X_t} \tag{8}$$

Since $C_1 \rightarrow C_4$ can be calculated from the geometry of the system, each possible location of the c.g. can be made to yield theoretical values for the 12 measurements. The c.g. is selected from these possible locations by comparing these theoretical values to the actual measured loads using a least-squares criterion.

$$\begin{bmatrix} X \\ Y \\ Z \end{bmatrix}_{\text{c.g.}} = \begin{bmatrix} \Sigma c_{1i}^2 & \Sigma c_{1i}c_{2i} & \Sigma c_{1i}c_{3i} \\ & \Sigma c_{2i}^2 & \Sigma c_{2i}c_{3i} \\ \text{Sym.} & & \Sigma c_{3i}^2 \end{bmatrix}^{-1} \begin{bmatrix} \Sigma c_{1i}\left(\frac{W_i}{W_t} - c_{4i}\right) \\ \Sigma c_{2i}\left(\frac{W_i}{W_t} - c_{4i}\right) \\ \Sigma c_{3i}\left(\frac{W_i}{W_t} - c_{4i}\right) \end{bmatrix} \tag{9}$$

where:

W_i = measured value for ith orientation

In the moment of inertia procedures, the theoretical value of the period of the rotational motion of the trifilar pendulum is

$$T = \left[\frac{I_{33}p \cdot c}{mg}\right]^{1/2} 2\pi \tag{10}$$

as developed in Appendix F. or

$$T^2 = I_{33}\,\frac{c}{mg}\,4\pi^2 p \tag{11}$$

The value of I_{33} in these measurements is a function of the jig inertial tensor and the orientation.

$$I_{33}\text{ procedures} = [t_{31n}t_{32n}t_{33n}]\begin{bmatrix} I_{11} & I_{12} & I_{13} \\ I_{21} & I_{22} & I_{23} \\ I_{31} & I_{32} & I_{33} \end{bmatrix}_{\text{jig}}\begin{bmatrix} t_{31n} \\ t_{32n} \\ t_{33n} \end{bmatrix} \tag{12}$$

Since $I_{21} = I_{12}, I_{31} = I_{13}, I_{23} = I_{32}$. This equation can be combined with the equation for the period to yield

$$T_n^2 = c_{1n}I_{11} + c_{2n}I_{12} + c_{3n}I_{13} + c_{4n}I_{22} + c_{5n}I_{23} + c_{6n}I_{33} \tag{13}$$

where $c_{1n} - c_{6n}$ are functions of the system geometry and the location of the c.g.

A least-squares solution is complicated by the fact that T_n is the quantity measured while T_n^2 is the quantity mobilized in these equations. However, taking advantage of

$$\begin{aligned}(T_n^2\text{ theoretical} - T_n^2\text{ measured})^2 &= (T_n\text{ theoretical} - T_n\text{ measured})^2 \\ &\quad (T_n\text{ theoretical} + T_n\text{ measured})^2 \\ &\cong (T_n\text{ theoretical} - T_n\text{ measured})^2\ 4\,T_n^2\text{ measured}\end{aligned}$$

and minimizing the term

$$(T_n^2\text{ theoretical} - T_n^2\text{ measured})^2/4T_n^2\text{ measured}$$

yields (14)

$$\begin{bmatrix} I_{11} \\ I_{12} \\ I_{13} \\ I_{22} \\ I_{23} \\ I_{33} \end{bmatrix}\begin{bmatrix} \Sigma_n \dfrac{(c_{1n})^2}{T_n^2} & \Sigma_n \dfrac{(c_{1n}c_{2n})}{T_n^2} \cdots\cdots \\ \cdot & \cdot \\ \cdot & \cdot \\ \cdot & \cdot \\ \cdot & \cdot \\ \cdot & \cdot \end{bmatrix}^{-1}\begin{bmatrix} \Sigma_n c_{1n} \\ \cdot \\ \cdot \\ \cdot \\ \cdot \\ \cdot \end{bmatrix} \tag{15}$$

The results of the least-squares procedures for both the c.g. vector and the moment of inertia tensor can then be used to calculate theoretical values for each of the quantities measured. Comparing these will show which measurements, if any, involve procedural or transcriptive errors.

These measurements are then eliminated from the summations in a second application of the least-squares procedures.

Once these procedures have yielded the inertia tensor and the c.g. vector for the empty jig and for the subject jig combination, all that remains is to extract these quantities for the subject alone.

The subject c.g. is given by

$$x_{\text{c.g.},s} = \frac{1}{w_s}\left[w_{sj}x_{\text{c.g.},sj} - w_j x_{\text{c.g.},j}\right] \tag{16}$$

$$\left.\begin{matrix} y_{\text{c.g.},s} \\ z_{\text{c.g.},s} \end{matrix}\right\} \text{ similarly}$$

The subject inertia tensor is given by

$$I_{11s} = I_{11sj} - I_{11j} + \frac{1}{g}\left[w_{sj}\left(y_{\text{c.g.}}{}^2{}_{sj} + z_{\text{c.g.}}{}^2{}_{sj}\right) - w_s\left(y_{\text{c.g.}}{}^2{}_s + z_{\text{c.g.}}{}^2{}_s\right) - w_j\left(y_{\text{c.g.}}{}^2{}_j - z_{\text{c.g.},j}\right)^2\right] \tag{17}$$

$$I_{12s} = I_{12sj} - I_{12j} - \left[w_{sj}\left(x_{\text{c.g.},sj}\,y_{\text{c.g.},sj}\right) - w_s\left(x_{\text{c.g.},s}\,y_{\text{c.g.},s}\right) - w_j\left(x_{\text{c.g.},j}\,y_{\text{c.g.},j}\right)\right] \tag{18}$$

and so on.

The values are expressed in the jig coordinate system and are transformed to the subject coordinates as follows:

$$\begin{bmatrix} x_{\text{c.g.},s} \\ y_{\text{c.g.},s} \\ z_{\text{c.g.},s} \end{bmatrix}_{\substack{\text{subject} \\ \text{coordinates}}} = \begin{bmatrix} \iota_{ij} \end{bmatrix}^T \left(\begin{bmatrix} x_{\text{c.g.},s} \\ y_{\text{c.g.},s} \\ z_{\text{c.g.},s} \end{bmatrix}_{\substack{\text{jig} \\ \text{coordinates}}} - \begin{bmatrix} b_1 \\ b_2 \\ b_3 \end{bmatrix} \right) \tag{19}$$

$$[I_{ls}]_{\text{subject}} = [\iota_{ij}]^T [I_{ls}]_{\text{jig}} [\iota_{ij}] \tag{20}$$

where ι_{ij} and b_i are the transformation parameters in Eq. 1.

Calibration

A number of small weights were attached to the jig to simulate a body of known c.g. and moment of inertia. These quantities were then measured using the procedures described in this paper.

The results of the moment of inertia procedures were then used to determine empirically an operational value for p the length of the wires in the trifilar pendulum.

The c.g. of the weight-jig system and of the empty jig was calculated, and the

SUBJECT NUMBER xxxx WEIGHT xxxx

MOMENT OF INERTIA C.G.

I_{11}	I_{12}	I_{13}	x_{cc}
.	.	.	y_{cc}
.	.	.	z_{cc}

PRINCIPAL AXES			MOMENTS	SEMI AXES
t_{11}	t_{12}	t_{13}	I_1	a
.	.	.	I_2	b
.	.	.	I_3	c

All numbers in Fortran floating point or exponential notation the significant digits convention is not followed

SUBJECT NUMBER 3356 (Head) WEIGHT 4420.2579 (gm)

MOMENT OF INERTIA (kg-m²) C.G. (cm)

.218851-01	-.282909-03	.466125-02	1.015377
-.282909-03	.279417-01	.622027-03	-.121901
.466125-02	.622027-03	.189044-01	2.244540

PRINCIPAL AXES			MOMENTS (kg-m²)	SEMI AXES (cm)
.808635	-.051046	.586092	.252814-01	10.14
.009794	.997259	.073343	.279846-01	9.50
-.588229	-.053558	.806918	.154652-01	14.62

SUBJECT NUMBER 3152 (Head) WEIGHT 3324.8300 (gm)

MOMENT OF INERTIA (kg-m²) C.G. (cm)

.101996-01	.336626-04	-.792482-03	1.217777
.336626-04	.140676-01	.360824-03	-.149448
-.792482-03	.360824-03	.135011-01	4.654642

PRINCIPAL AXES			MOMENTS (kg-m²)	SEMI AXES (cm)
.974090	-.028081	.22441	.100160-01	11.55
-.089472	.363463	.496413	.142715-01	8.33
-.207710	-.503629	.838579	.134807-01	9.01

SUBJECT NUMBER 2986 (Head) WEIGHT 4406.6499 (gm)

MOMENT OF INERTIA (kg-m²) C.G. (cm)

.221516-01	.931637-03	.537359-02	1.182619
.931637-03	.266541-01	-.117163-03	-.273127
.537359-02	-.117163-03	.181217-01	1.728442

PRINCIPAL AXES			MOMENTS (kg-m²)	SEMI AXES (cm)
.696214	-.498198	.516803	.254737-01	9.52
.434483	.865555	.249078	.270880-01	8.51
-.571411	.051130	.819070	.143656-01	14.72

Fig. 4 - Sample charts

SUBJECT NUMBER 3121 (Head) WEIGHT 3533.4850 (gm)

MOMENT OF INERTIA (kg-m²)			C.G. (cm)
.147954-01	.657236-04	.342656-02	1.403023
.657236-04	.199531-0'	.653389-03	-.062807
.342656-02	.653389-03	.141152-01	1.897174

PRINCIPAL AXES			MOMENTS (kg-m²)	SEMI AXES (cm)
.732939	-.217067	.644735	.177905-01	9.69
.129457	.974914	.181063	.200831-01	7.84
-.667564	-.049243	.742653	.109904-01	13.79

SUBJECT NUMBER 3129 (Head) WEIGHT 3727.3950 (gm)

MOMENT OF INERTIA (kg-m²)			C.G. (cm)
.175926-01	-.13?226-03	.275139-02	1.222075
-.13?226-03	.199732-01	.250295-03	.111047
.275239-02	.250295-03	.131853-01	- [illegible]

PRINCIPAL AXES			MOMENTS (kg-m²)	SEMI AXES (cm)
.901020	.015151	.433513	.189147-01	9.31
-.028?79	.999269	.025099	.199835-01	8.50
-.432515	-.035134	.900798	.118531-01	13.47

SUBJECT NUMBER 3343 (Head) WEIGHT 4209.3369 (gm)

MOMENT OF INERTIA (kg-m²)			C.G. (cm)
.183249-01	-.341270-03	.371126-02	1.821289
-.341270-03	.220194-01	.943651-03	-.076566
.371126-02	.943651-03	.175590-01	2.142644

PRINCIPAL AXES			MOMENTS (kg-m²)	SEMI AXES (cm)
.742537	-.204301	.637887	.216070-01	9.65
.090078	.974155	.207144	.231686-01	8.64
-.663720	-.09653	.741749	.141278-01	13.49

SUBJECT NUMBER 1000003343 (Head, Neck) WEIGHT 5910.3079 (gm)

MOMENT OF INERTIA (kg-m²)			C.G. (cm)
.340734-01	.105?67-02	- 221405-02	.3?1794
-.105?67-02	.432936-01	.951545-03	-.252?41
-.221405-02	.951545-03	.272521-01	-.193519

PRINCIPAL AXES			MOMENTS (kg-m²)	SEMI AXES (cm)
.951?7?	.144522	-.270261	.345413-01	12.26
-.129?13	.9??9?9	?75430	435040-01	8.62
.27?13?	-.037014	.95?[illegible]	.265738-01	14.75

SUBJECT NUMBER 1000003326 (Head, Neck) WEIGHT 5527.0229 (gm)

MOMENT OF INERTIA (kg-m²)			C.G. (cm)
.314966-01	.7?6?84-03	-.103?29-02	-.340163
.7?6?84-03	.425?83-01	.692953-04	.229506
-.103?29-02	.692953-04	.254380-01	.726336

PRINCIPAL AXES			MOMENTS (kg-m²)	SEMI AXES (cm)
.9?3666	-.069402	- 166086	.316163-01	12.81
.070342	.997523	-.000221	.426439-01	8.02
.165690	- 011463	.9?6111	.252627-01	14.89

SUBJECT NUMBER 1000003356 (Head, Neck) WEIGHT 6044.1179 (gm)

MOMENT OF INERTIA (kg-m²)			C.G. (cm)
.409030-01	.772226-03	-.335993-02	-1.114?6?
.772226-03	.?94396-01	.3143?4-03	.061522
-.335993-02	.3143?4-03	.261?02-01	- .493694

PRINCIPAL AXES			MOMENTS (kg-m²)	SEMI AXES (cm)
.972?94	-.0?7301	-.214139	.415735-01	11.75
.0?9?15	.995?9?	.000509	.495089-01	8.51
.213235	-.019657	.976803	.254404-01	16.4?

Fig 4 - Sample charts

c.g. was used to calculate theoretical values for the weights measured at the projections. As expected, these theoretical values differed in a uniform manner from the measured quantities. The uniformity of the difference and the symmetry of the experiments lead one to believe that these errors are self-canceling.

Similarly, the moment of inertia tensors of these systems were calculated and then used to calculate theoretical periods of oscillation. These theoretical values also differed in a uniform manner from the measured quantities.

The reason for this difference is caught up in the mechanics of the jig hangings. There is a slight difference in the geometry when the jig is hung from the projections of three vertexes as opposed to when it is hung from projections of two vertexes and an edge-midpoint.

Although the measurements performed on the series of weights were used to calibrate the device, since only a single calibration constant was sought, the results of these measurements indicate the workability of the method.

The position of the c.g. determined by the measurements was displaced about 1/2 cm from its true location. Since the mass of the subjects for which this approach is intended is on the order of three times greater than the mass involved here, one would expect that the positions of the c.g. as calculated would be within 2 mm of their true positions.

The moment of inertia of the series of weights can be visualized as a perfect sphere. The calculated moment of inertia is then a sphere so slightly deformed that its smallest and largest diameters are each within 1% of the true value.

Results

The procedures were applied to nine subjects, six heads, and three head-and-necks at Tulane Medical School during October 5–23, 1971. The following measurements were made for each subject:

1. Subject weight.
2. Locations of right and left auditory meatuses in the jig.
3. Locations of right and left orbital notches in the jig.
4. Location of anterior nasal spine in the jig.
5. Weight distribution of projections for subject-jig system.
6. Weight distribution to projections for empty jig.
7. Periods of rotational oscillation for subject-jig system.
8. Periods of rotational oscillation for empty jig.

These were input to a computer program embodying the manipulations developed in the mathematics section to solve for:

1. The c.g. vector.
2. The moment of inertia tensor.
3. The principal moments.
4. The alignments of these moments.

The value of the measurements taken on the six heads and the three head-and-necks is questionable. The weights of the heads dropped as much as 25% from the time the anatomical sections were made to the time of the measurements. This weight loss is due largely to dehydration in that even though the subjects were immersed in liquid preservative, the tissues lost their fluids and became leathery.

Although this dehydration could not be expected to affect all tissues uniformly, massless parameters of the subject mass distribution would be less altered and thus more reliable indicators of the actual in vivo situation than those involving

mass. For example, the c.g. vector would probably be more reliable than the weight. The alignments of the principal moments of inertia would probably be more reliable than the values of those principal moments.

For this reason, there are tabulated, along with the principal moments of each subject, the lengths of the semiaxes of an ellipsoidal body of uniform density having the same mass and moments of inertia. These parameters are similar but not identical to the radius of gyration often calculated for bodies in rotation about a single axis.

The data for each subject include the three-by-three moment of inertia tensor, the three components of the c.g. vector, a direction cosine matrix composed of three row vectors of the principal axes of the moment of inertia tensor, the three principal moments, and the three semiaxes (Fig. 4).

Although the sample size in each case is too small to validate statistically any strong conclusions, the results indicate the following:

1. The data on head 3152 are anomalous.
2. The human head and head-and-neck are roughly symmetrical about the midsagittal plane.
3. The anatomical reference points used to locate the head-referenced coordinates are sufficiently indicative of the mass distribution of the head and head-and-

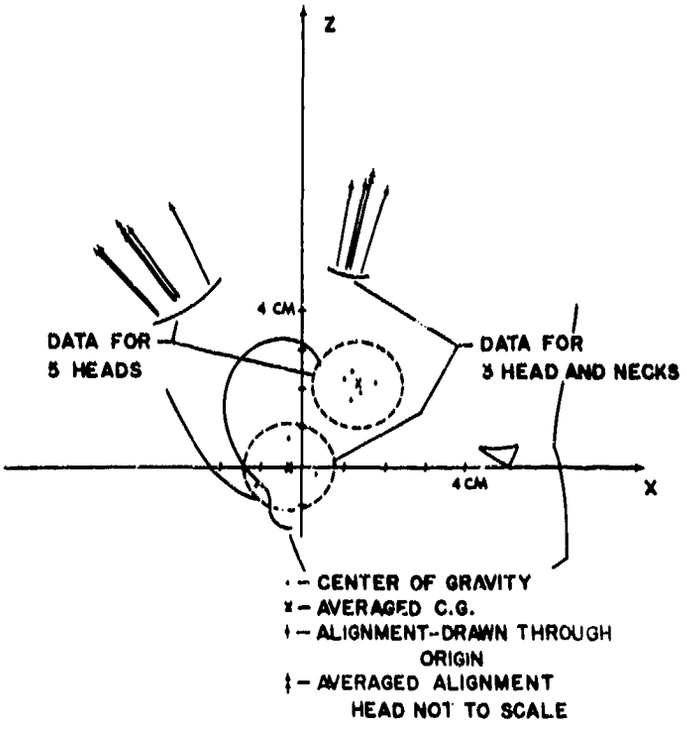

Fig. 5 - Alignments of I_{zz} principal axis and c.g. in head-referenced X–Z (midsaggital) plane

neck that when these data are described in terms of these coordinates, there is a noticeable correlation between subjects. This is illustrated in Fig. 5, which shows the c.g. and the alignments of the z principal moment in the midsagittal plane.

In the future, load cells will be substituted for the scale in the c.g. procedures affording accurate load distributions. A new hanging arrangement will be used in the moment of inertia procedures allowing a much more accurate determination of the geometries. These updated procedures will then be applied to as many subjects as possible.

The problem of weight losses in the cadaveric material, while probably not insurmountable, is probably so dependent upon embalming techniques that the only workable solution would be to insist on the remains of the recently departed.

These procedures can be readily adapted to other anatomical segments. The tetrahedral jig can be built to the largest scale necessary without any radical changes in its structure. Once suitable devices to hold the subject segment within the jig are fabricated, and the measurements and algorithms necessary to locate a three-dimensional coordinate system within that segment formulated, all that remains is to apply the two sets of procedures given here to determine the c.g. vector and the moment of inertia tensor.

Nomenclature

b_n = nth component of vector displacement
C_n, c_n = nth constant in many equations (second subscript indicates system orientation)
g = acceleration due to gravity (positive down)
ι_{nm} = direction cosine between nth coordinate in one system and mth coordinate in another
m = system mass
p = length of pendulum wires
T = rotational period
w = weight
x, y, z = cartesian coordinates
n,m,l = coordinates, orientations, or entries in equation
c.g. = center of gravity
jig, j, J = jig
s, head = subject
sj = subject-jig combination
x = operator for vector cross-product
T = matrix transpose
$\wedge$ = unit vector

Acknowledgments

This work was funded by the U.S. Navy Bureau of Medicine and Surgery and the Medical and Dental Division of the Office of Naval Research. Opinions or conclusions contained in this report do not necessarily reflect the views or endorsement of the Navy Department.

Trade names of materials or products of commercial or nongovernment organizations are cited only where essential to precision in describing research proce-

dures or evaluation of results. Their use does not constitute official endorsement or approval of the use of such commercial hardware or software.

To Gloria Bourgeois, who assisted in the preparation of this report; to Leon Walker and Uwe Pontius of the Tulane University Medical School, who provided the anatomical segments and gave freely of their time and advice; to William Decker and Frederick Walgis of the Naval Air Rework Facility, NAS Pensacola, who assisted in the design and fabrication of the tetrahedral frame; to Bobby Teal and Willard Hunt, who assisted in the measurements; and to Channing L. Ewing, Daniel J. Thomas, Gilberto Willems, William Muzzy, and William Anderson, the author extends his most grateful appreciation.

Reference

1. Walker, et al., A Letter Report Under ONR Contract N00014-69-A-0248-0001, Tulane University Medical School, Department of Anatomy, November 1971.

Appendix A

The dynamic equation of a balance scale (Fig. A-1) is

$$I\ddot{\phi} + b\dot{\phi} + (f_1 + f_2)\,d\phi + (f_2 l_2 - f_1 l_1) = 0 \qquad d \ll l_1, l_2 \tag{A-1}$$

where:

I = system inertia
b = system damping
f_2 = weight being measured
f_1 = calibrated weight used in measurement

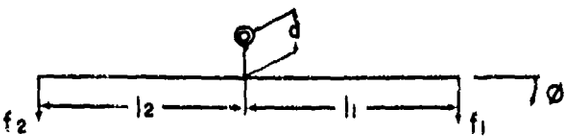

Fig. A-1 - Balance scale

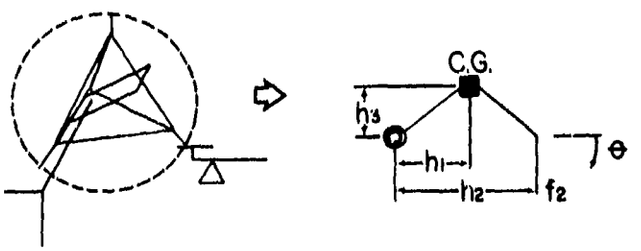

Fig. A-2 - Projection loadings

d, the offset of the pivot from the lever arm, guarantees that the arm will oscillate to a stable equilibrium at $\phi = 0$ whenever $f_2 = f_1$.

However, in the case of the c.g. procedures (Fig. A-2), f_2 is not constant with ϕ

$$\begin{aligned} f_2 &= fm(h_1 + h_3\theta)/h_2 \\ \theta h_2 &= -\phi\, \iota_2 \\ d &\ll h_1, h_2, h_3 \end{aligned} \tag{A-2}$$

This means that for small oscillations, the dynamic equation of the scale is

$$\begin{aligned} I\ddot{\phi} + b\dot{\phi} - (fm\, h_3\, \iota_2^2/h_2^2 - f_1 d - fm\, h_1 d/h_2)\phi \\ + (fm\, h_1\, \iota_2/h^2 - f_1\iota_1) = 0 \end{aligned} \tag{A-3}$$

Since the term for ϕ in this equation is negative, the balance arm has no stable position and will always move toward one of its limits.

As an alternative, the test setup was arranged so that the jig was level when the balance pan was at its higher limit and the balance arm, consequently, at its lower limit. The reading at which this arrangement is no longer stable is equal to the load on the balance pan times some constant fixed in the scale geometry. This constant is

$$f_2 \text{ reading} = f_1 \frac{\iota_1}{\iota_2} = f_2 \left(1 + \frac{\iota_1 d\Delta + \iota_2 d\Delta}{\iota_2\iota_1 - \iota_2 d\Delta}\right) \tag{A-4}$$

where:

Δ = angle of balance arm at its lower limit

This small error is further alleviated by the least-squares solution to 12 measurements distributed symmetrically about the jig.

Nomenclature -

I = system inertia
b = system damping
d = offset of balance arm from its pivot
ϕ = angular position of balance arm
f_2, f_m = weight being measured
f_1 = calibrated counterweight
ι_1, ι_2 = lengths of balance lever arms
θ = angular position of jig
h_1, h_2, h_3 = lengths in jig geometry
$\cdot$ = differentiation with respect to time
$\cdot\cdot$ = double differentiation with respect to time

Appendix B

Given four points in three-dimensional space: $(X_1, Y_1, Z_1), \ldots, (X_4, Y_4, Z_4)$. The midpoint of a line joining any pair of these points is given by

$$\left.\begin{aligned} X_{ij} &= (X_i + X_j)/2 \\ Y_{ij} \\ Z_{ij} \end{aligned}\right\} \text{ similarly} \qquad \text{(B-1)}$$

where p_{ij} is the midpoint of the line joining point p_i to point p_j. Applying these equations, one can determine $p_{12}, p_{23}, p_{34}, p_{41}$.

A further application yields the midpoints of the lines joining p_{12} to p_{34} and p_{41} to p_{23}, and these midpoints are identical, being

$$\begin{aligned} &(X_1 + X_2 + X_3 + X_4)/4 \\ &\text{etc.} \\ &\text{etc.} \end{aligned} \qquad \text{(B-2)}$$

Thus, these two lines intersect so that p_{12}, p_{23}, p_{34}, and p_{41} must be coplanar.

Appendix C

The values for ι_{13} and b_1 are computed from the X, Y, and Z positions of the four anatomical landmarks as measured in the jig coordinates.

Let (X_1, Y_1, Z_1) and (X_2, Y_2, Z_2) be the jig-referenced positions of the right and left auditory meatuses, respectively, and (X_3, Y_3, Z_3) and (X_4, Y_4, Z_4) are the jig-referenced positions of the right and left orbital notches.

Then

$$\begin{aligned} b_1 &= (X_1 + X_2)/2 \\ b_2 &= (Y_1 + Y_2)/2 \\ b_3 &= (Z_1 + Z_2)/2 \end{aligned} \qquad \text{(C-1)}$$

and

$$\begin{aligned} \iota_{11} &= (X_3 + X_4 - X_1 - X_2)/\alpha \\ \iota_{21} &= (Y_3 + Y_4 - Y_1 - Y_2)/\alpha \\ \iota_{31} &= (Z_3 + Z_4 - Z_1 - Z_2)/\alpha \end{aligned} \qquad \text{(C-2)}$$

where:

$$\begin{aligned} \alpha &= [(X_3 + X_4 - X_1 - X_2)^2 + (Y_3 + Y_4 - Y_1 - Y_2)^2 \\ &\qquad + (Z_3 + Z_4 - Z_1 - Z_2)^2]^{1/2} \\ \iota_{13} &= [(\iota_{21}(Z_2 + Z_4 - Z_3 - Z_1) + \iota_{31}(Y_2 + Y_3 - Y_2 - Y_4)]/\beta \\ \iota_{23} &= [\iota_{31}(X_2 + X_4 - X_1 - X_3) + \iota_{11}(Z_1 + Z_3 - Z_2 - Z_4)]/\beta \\ \iota_{33} &= [\iota_{11}(Y_2 + Y_4 - Y_1 - Y_3) + \iota_{21}(X_1 + X_3 - X_2 - X_4)]/\beta \end{aligned} \qquad \text{(C-3)}$$

where:

$$\beta = \left[\{\iota_{21}(Z_2 + Z_4 - Z_3 - Z_1) + \iota_{31}(Y_1 + Y_3 - Y_2 - Y_4)\}^2 + \{\iota_{31}(X_2 + X_4 - X_1 - X_3) + \iota_{11}(Z_1 + Z_3 - Z_2 - Z_4)\}^2 + \{\iota_{11}(Y_2 + Y_4 - Y_1 - Y_3) + \iota_{21}(X_1 + X_3 - X_2 - X_4)\}^2\right]^{1/2} \quad \text{(C-4)}$$

and

$$\begin{aligned} \iota_{12} &= \iota_{23}\iota_{31} - \iota_{21}\iota_{33} \\ \iota_{22} &= \iota_{33}\iota_{11} - \iota_{13}\iota_{31} \\ \iota_{32} &= \iota_{13}\iota_{21} - \iota_{11}\iota_{23} \end{aligned} \quad \text{(C-5)}$$

where:

X_n, Y_n, Z_n = three components of position of point n in jig
b_n = nth component of position of origin of head coordinates
ιnm = direction cosine of alignment of nth jig coordinate to mth head coordinate
$\alpha\beta$ = quantities calculated in development for normalizing direction cosine but of no permanent interest

Appendix D

The X Y Z positions of the four anatomical landmarks in the jig coordinate system are obtained with the DKI 1760 micromanipulator (Fig. D-1). This highly flexible device has five measurements to be read for each setting and can be used in four different configurations.

It is composed of a base designed to attach to either of the two calibrated bars that make up the bulk of the DKI stereotaxic unit. The base can be moved along the length of these bars and is verniered to give its position on the bar to tenths of

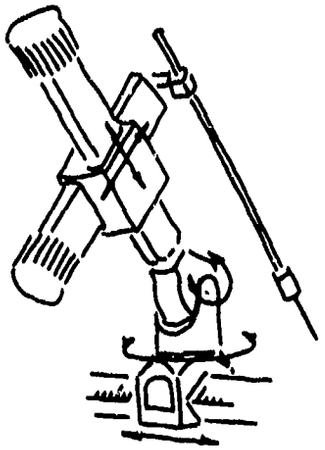

Fig. D-1 - DKI 1760 micromanipulator

millimetres. The base also provides angular adjustment and readout in two planes to a socket in which fits the other major component of the micromanipulator. This component is a pair of arms of variable and readable length set perpendicular to each other. The end of the first of these arms is set in any of four ways into the socket in the base of the manipulator. A pointer is attached to the end of the second arm.

The position of the end of the pointer relative to the end of the second arm is given by

$$\begin{bmatrix} C_1 \\ C_2 \\ C_3 \end{bmatrix} \tag{D-1}$$

to the socket end of the first arm

$$\begin{bmatrix} C_1 \\ C_2 \\ C_3 \end{bmatrix} + \begin{bmatrix} C_4 \\ C_5 - X_3 \\ C_6 - X_2 \end{bmatrix} \tag{D-2}$$

where X_2 and X_3 are the readings from the first and second arms, respectively.

The position with respect to the socket is then

$$\begin{bmatrix} A_n & -B_n & 0 \\ B_n & A_n & 0 \\ 0 & 0 & 1 \end{bmatrix} \begin{bmatrix} C_1 + C_4 \\ C_2 + C_5 - X_3 \\ C_3 + C_6 + X_2 \end{bmatrix} \tag{D-3}$$

where A_n and B_n are determined by the orientation of the arms to the base.

Orientation	A_n	B_n
1	1	0
2	0	−1
3	−1	0
4	0	1

To the front edge of the base

$$\begin{bmatrix} \cos\phi_1 & \cos\phi_2 & -\sin\phi_1 & \cos\phi_1 & \sin\phi_2 \\ \sin\phi_1 & \cos\phi_2 & \cos\phi_1 & \sin\phi_1 & \sin\phi_2 \\ -\sin\phi_2 & & 0 & \cos\phi_2 & \end{bmatrix} \begin{bmatrix} A_n & -B_n & 0 \\ B_n & A_n & 0 \\ 0 & 0 & 1 \end{bmatrix} \begin{bmatrix} C_1 + C_4 \\ C_2 + C_5 - X_3 \\ C_3 + C_6 + X_5 \end{bmatrix}$$

(D-4)

where ϕ_1 and ϕ_2 are the angular readings at the first and second pivots.

In the jig coordinates for the bar on the right,

$$\begin{bmatrix} \cos\phi_1 & \cos\phi_2 \cdots \\ \cdot & \\ \cdot & \\ \cdot & \end{bmatrix} \begin{bmatrix} A_n \cdots \\ \cdot \\ \cdot \\ \cdot \end{bmatrix} \begin{bmatrix} C_1 + C_4 \\ C_2 + C_5 - X_3 \\ C_3 + C_6 + X_5 \end{bmatrix} + \begin{bmatrix} C_7 + X_1 \\ C_8 \\ C_9 \\ \end{bmatrix} \tag{D-5}$$

For the bar on the left,

$$\begin{bmatrix} -1 & 0 & 0 \\ 0 & -1 & 0 \\ 0 & 0 & 1 \end{bmatrix} \cdot \begin{bmatrix} \cos\phi_1 & \cos\phi_2 \cdots \\ & \cdot \\ & \cdot \end{bmatrix} \cdot \begin{bmatrix} A_n \cdots \\ \cdot \\ \cdot \end{bmatrix} \begin{bmatrix} C_1 + C_4 \\ C_2 + C_5 - X_3 \\ C_3 + C_6 + X_5 \end{bmatrix} + \begin{bmatrix} C_7 + X_1 \\ C_{10} + C_8 \\ C_9 \end{bmatrix} \tag{D-6}$$

These expressions can be simplified to:

For the bar on the right

$$\begin{bmatrix} \cos\phi_1 & \cos\phi_2 \cdots \\ \cdot & \\ \cdot & \end{bmatrix} \cdot \begin{bmatrix} A_n \cdots \\ \cdot \\ \cdot \end{bmatrix} \cdot \begin{bmatrix} C_1 \\ C_2 - X_3 \\ C_3 + X_2 \end{bmatrix} + \begin{bmatrix} C_4 + X_1 \\ C_5 \\ C_6 \end{bmatrix} \tag{D-7}$$

For the bar on the left:

$$\begin{bmatrix} -1 & 0 & 0 \\ 0 & -1 & 0 \\ 0 & 0 & 1 \end{bmatrix} \cdot \begin{bmatrix} \cos\phi_1 & \cos\phi_2 \cdots \\ \cdot & \\ \cdot & \end{bmatrix} \cdot \begin{bmatrix} A_n \cdots \\ \cdot \\ \cdot \end{bmatrix} \cdot \begin{bmatrix} C_1 \\ C_2 - X_3 \\ C_3 + X_2 \end{bmatrix} + \begin{bmatrix} C_4 + X_1 \\ C_5 + C_7 \\ C_6 \end{bmatrix} \tag{D-8}$$

where:

C_n = lengths encountered in system hardware
x_1 = reading giving position of manipulator on jig
x_2 = reading taken on first arm
x_3 = reading taken on second arm
ϕ_1 = angular position about first pivot
ϕ_2 = angular position about second pivot
A_n, B_n = constants determined by system configuration

C_1 C_7 are constants determined by the hardware. $X_1, \phi_1, \phi_2, X_2, X_3$ are the readings for the manipulator in order from the base to the pointer.

Appendix E

The moment of inertia procedures involve measurements of the dynamic behavior of a trifilar pendulum. A trifilar pendulum consists of a rigid body suspended by three wires of equal length attached to congruent points in the body and in a plane fixed perpendicular to gravity.

A complete statement of just the kinematics of such a system would be quite complex and is beyond the scope of this paper. However, the kinematics for small transverse and rotational displacements from the equilibrium position can be approximated in the following manner.

Assume a rigid body suspended by three wires. Each of length P attached to congruent points in the body A, B, and C and a plane fixed perpendicular to gravity. The equilibrium position then has the plane of A, B, and C parallel to the fixed plane and each of the three wires parallel to the gravity vector if the perpendicular from the c.g. to the plane A, B, C passes through the triangle $A\ B\ C$.

If the wires are not permitted to go slack, this system has three degrees of freedom. The position and orientation of the body in space for small displacements (Fig. E-1) from the equilibrium condition can be described as functions of the displacement of the body in a plane perpendicular to gravity and rotation about an axis parallel to gravity.

Assume a right-handed coordinate system located in the body with the origin at A, the Y-axis passing through B, and the XY plane including C such that X is positive toward C.

Assume a similar coordinate system located in the laboratory such that the lab and body coordinates overlap perfectly when the body is in its equilibrium position.

Given small displacements of the body relative to the lab in x and y and small rotations ϕ about the body z-axis, the displacement of A, B, and C in the lab

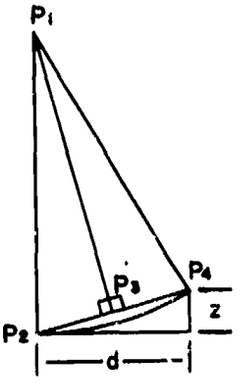

$$\overline{P_1P_2} = \overline{P_1P_4} = P \gg d$$

$$\frac{z}{d} = \frac{\overline{P_2P_3}}{\overline{P_1P_3}} \approx \frac{d/2}{P}$$

$$z \approx \frac{d^2}{2P}$$

Fig. E-1 - Vertical motion for small displacements

x-y plane are

$$\begin{aligned}\vec{d}_A &= \vec{x} + \vec{y}\\ \vec{d}_B &= (x - Y_B\phi)\hat{x} + \vec{y}\\ \vec{d}_C &= (x - Y_C\phi)\hat{x} + (y + X_C\phi)\hat{y}\end{aligned} \tag{E-1}$$

Where x, y, ϕ represent the displacements and X, Y represent points fixed in the body coordinates.

The z displacements of A, B, and C can be approximated using the geometry in the figure

$$z_A = \frac{(\vec{d}_A)^2}{2p} \tag{E-2}$$

$$\left.\begin{matrix} z_B \\ z_C \end{matrix}\right\} \text{ similarly}$$

Rotation about the x axis is

$$\theta_1 \cong \tan^{-1}\frac{(z_B - z_A)}{Y_B} \cong \frac{z_B - z_A}{Y_B} \tag{E-3}$$

Rotation about the y axis is

$$\theta_2 = \frac{\theta_1 Y_C + z_A - z_C}{X_C} \tag{E-4}$$

The displacements at the c.g. are then

$$\begin{aligned}x_{\text{c.g.}} &= x - \phi Y_{\text{c.g.}} + \theta_2 Z_{\text{c.g.}}\\ y_{\text{c.g.}} &= y + \phi X_{\text{c.g.}} - \theta_1 Z_{\text{c.g.}}\\ z_{\text{c.g.}} &= z_A + \theta_1 X_{\text{c.g.}} - \theta_2 X_{\text{c.g.}}\end{aligned} \tag{E-5}$$

Combining equations to obtain these quantities in terms of x, y, ϕ and the system geometry,

$$\begin{aligned}\theta_1 &= \frac{Y_B}{2p}\phi^2 - \frac{1}{p}\phi x\\ \theta_2 &= \frac{1}{2p}\left[\frac{Y_C^2 + X_C^2 - Y_B Y_C}{X_C}\right]\phi^2 - \frac{1}{p}\phi y\\ x_{\text{c.g.}} &= x - \phi Y_{\text{c.g.}} - \frac{Z_{\text{c.g.}}}{2p}\frac{Y_C^2 + X_C^2 - Y_B Y_C}{X_C}\phi^2 - \frac{Z_{\text{c.g.}}}{p}\phi y\\ y_{\text{c.g.}} &= y + \phi X_{\text{c.g.}} - \frac{Z_{\text{c.g.}}}{2p}Y_B\phi^2 + \frac{Z_{\text{c.g.}}}{p}\phi x\\ z_{\text{c.g.}} &= \frac{1}{2p}[x^2 + y^2] + \frac{Y_{\text{c.g.}} Y_B}{2p}\phi^2 - \frac{Y_{\text{c.g.}}}{p}\phi x\\ &\quad + \frac{X_{\text{c.g.}}}{2p}\left[\frac{Y_C^2 + X_C^2 - Y_B Y_C}{X_C}\right]\phi^2 + \frac{X_{\text{c.g.}}}{p}\phi y\end{aligned} \tag{E-6}$$

or

$$\begin{aligned}
\phi &= -- \\
\theta_1 &= c_1\phi^2 - c_2\phi x \\
\theta_2 &= c_3\phi^2 + c_2\phi y \\
x_{c.g.} &= x + c_4\phi + c_5\phi^2 + c_6\phi y \\
y_{c.g.} &= y + c_7\phi + c_8\phi^2 + c_6\phi x \\
z_{c.g.} &= c_9[x^2 + y^2] + c_{10}\phi^2 + c_{11}\phi x + c_{12}\phi y
\end{aligned} \tag{E-7}$$

where c_1–c_{12} are all constants in the system geometry.

$$\begin{aligned}
c_1 &= \frac{Y_B}{2p}\, c_2 = \frac{1}{p} \\
c_3 &= -\frac{1}{2p}\,\frac{Yc^2 + Xc^2 - Y_B Y_C}{Xc} \\
c_4 &= Y_{c.g.} \\
c_5 &= Z_{c.g.} c_3 \\
c_6 &= \frac{Z_{c.g.}}{p} \\
c_7 &= X_{c.g.} \\
c_8 &= \frac{Z_{c.g.} Y_B}{2p} \\
c_9 &= \frac{1}{2p} \\
c_{10} &= \frac{1}{2p}\left[Y_{c.g.} YB + \frac{X_{c.g.}}{X_C}\,[Y_C^2 + X_C^2 - Y_B Y_C]\right] \\
c_{11} &= -\frac{Y_{c.g.}}{p} \\
c_{12} &= +\frac{X_{c.g.}}{p}
\end{aligned} \tag{E-8}$$

The dynamic equations for the system can now be developed from Hamilton's principle in the following manner. The kinetic coenergy (TE) of the system is

$$\begin{aligned}
TE = {} & 1/2\, m[\dot{x}_{c.g.}^2 + \dot{y}_{c.g.}^2 + \dot{z}_{c.g.}^2] \\
& + 1/2\,[I_{11}\dot{\theta}_1^2 + 2I_{12}\dot{\theta}_1\dot{\theta}_2 + I_{22}\dot{\theta}_2^2 \\
& + 2I_{13}\dot{\theta}_1\dot{\phi} + 2I_{23}\dot{\theta}_2\dot{\phi} + I_{33}\dot{\phi}^2]
\end{aligned} \tag{E-9}$$

and the potential energy is

$$v + mg\, z_{c.g.}$$

forming the integral

$$\int_{t_1}^{t_2} (\mathrm{TE} - v)dt$$

and applying the variational calculus yields

$$m\left[\ddot{x}_{c.g.}\frac{\partial x_{c.g.}}{\partial x} + \ddot{y}_{c.g.}\frac{\partial y_{c.g.}}{\partial x} + \ddot{z}_{c.g.}\frac{\partial z_{c.g.}}{\partial x}\right] + I_{11}\ddot{\theta}_1\frac{\partial \theta_1}{\partial x} + I_{12}\ddot{\theta}_1\frac{\partial \theta_2}{\partial x} + I_{12}\ddot{\theta}_2\frac{\partial \theta_1}{\partial x} + I_{22}\ddot{\theta}_2\frac{\partial \theta_2}{\partial x} + I_{13}\ddot{\phi}\frac{\partial \theta_1}{\partial x} + I_{23}\ddot{\phi}\frac{\partial \theta_2}{\partial x} + \mathrm{mg}\frac{\partial z_{c.g.}}{\partial x} = 0$$

$$m\left[\ddot{x}_{c.g}\frac{\partial x_{c.g.}}{\partial y} + \ddot{y}_{c.g.}\frac{\partial y_{c.g.}}{\partial y} + \ddot{z}_{c.g.}\frac{\partial z_{c.g.}}{\partial y}\right] + I_{11}\ddot{\theta}_1\frac{\partial \theta_1}{\partial y} + I_{12}\ddot{\theta}_1\frac{\partial \theta_2}{\partial y} + I_{12}\ddot{\theta}_2\frac{\partial \theta_1}{\partial y} + I_{22}\ddot{\theta}_2\frac{\partial \theta_2}{\partial y} + I_{13}\ddot{\phi}\frac{\partial \theta_1}{\partial y} + I_{23}\ddot{\phi}\frac{\partial \theta_2}{\partial y} + \mathrm{mg}\frac{\partial z_{c.g.}}{\partial y} = 0$$

$$m\left[\ddot{x}_{c.g.}\frac{\partial x_{c.g.}}{\partial \phi} + \ddot{y}_{c.g.}\frac{\partial y_{c.g.}}{\partial \phi} + \ddot{z}_{c.g.}\frac{\partial z_{c.g.}}{\partial \phi}\right] + I_{11}\ddot{\theta}_1\frac{\partial \theta_1}{\partial \phi} + I_{12}\ddot{\theta}_1\frac{\partial \theta_2}{\partial \phi} + I_{12}\ddot{\theta}_2\frac{\partial \theta_1}{\partial \phi} + I_{22}\ddot{\theta}_2\frac{\partial \theta_2}{\partial \phi} + I_{23}\ddot{\theta}_1 + I_{13}\ddot{\phi}\frac{\partial \theta_1}{\partial \phi} + I_{33}\ddot{\phi} + I_{23}\ddot{\theta}_2 + I_{23}\ddot{\phi}\frac{\partial \theta_2}{\partial \phi} + mg\frac{\partial z_{c.g.}}{\partial \phi} = 0 \qquad \text{(E-10)}$$

Substituting from the kinematic equations,

$$\begin{aligned}
&m\,[\ddot{x}_{c.g.} + c_6\phi\ddot{y}_{c.g.} + (2c_9x + c_{11}\phi)\ddot{z}_{c.g.}] \\
&\quad - I_{11}c_2\phi\ddot{\theta}_1 - I_{12}\ddot{\theta}_2c_2\phi \\
&\quad - I_{13}c_2\phi\ddot{\phi} + mg[2c_9x + c_{11}\phi] = 0 \\
&m\,[c_6\phi\ddot{x}_{c.g.} + \ddot{y}_{c.g.} + (2c_9y + c_{12}\phi)\ddot{z}_{c.g.}] \\
&\quad + I_{12}\ddot{\theta}_1c_2\phi + I_{22}\ddot{\theta}_2c_2\phi + I_{23}\ddot{\phi}c_2\phi \\
&\quad + mg[2c_9y + c_{12}\phi] = 0 \\
&m\,[(c_4 + 2c_5\phi + c_6x)\ddot{x}_{c.g.} + (c_7 + 2c_8\phi + c_6x)\ddot{y}_{c.g.} \\
&\quad + (2c_{10}\phi + c_{11}x + c_{12}y)\ddot{z}_{c.g.}] \\
&\quad + [I_{11}\ddot{\theta}_1 + I_{12}\ddot{\theta}_2 + I_{13}\ddot{\phi}][2c_1\phi - c_2x] \\
&\quad + [I_{22}\ddot{\theta}_2 + I_{12}\ddot{\theta}_1 + I_{23}\ddot{\phi}][2c_3\phi + c_2y] \\
&\quad + I_{33}\ddot{\phi} + I_{13}\theta_1 + I_{23}\theta_2 + mg[2c_{10}\phi + c_{11}x + c_{12}y] = 0
\end{aligned} \qquad \text{(E-11)}$$

Since all the displacement terms are small, products of these terms are insignificant. Eliminating these from the dynamic equations yields

$$\begin{aligned} m\ddot{x}_{c.g.} + mg[2c_9 x + c_{11}\phi] &= 0 \\ m\ddot{y}_{c.g.} + mg[2c_9 y + c_{12}\phi] &= 0 \\ c_4 m\ddot{x}_{c.g.} + c_7 m\ddot{y}_{c.g.} + I_{33}\ddot{\phi} + I_{13}\ddot{\theta}_1 + I_{23}\ddot{\theta}_2 & \\ + mg[2c_{10}\phi + c_{11}x + c_{12}y] &= 0 \end{aligned} \tag{E-12}$$

And from the kinematic equations

$$\begin{aligned} \phi &= — \\ \theta_1 &\simeq 0 \\ \theta_2 &\simeq 0 \\ x_{c.g.} &\simeq x + c_4\phi \\ y_{c.g.} &\simeq y + c_7\phi \\ z_{c.g.} &\simeq 0 \end{aligned} \tag{E-13}$$

Taking advantage of

$$\begin{aligned} 2c_9 x + c_{11}\phi &= \frac{1}{p}[x + c_4\phi] = x_{c.g.} \\ 2c_9 y + c_{12}\phi &= \frac{1}{p}[y + c_7\phi] = y_{c.g.} \\ c_{11} &= + \frac{c_4}{p} \quad c_{12} = \frac{c_7}{p} \end{aligned} \tag{E-14}$$

Gives

$$\begin{aligned} & m\ddot{x}_{c.g.} + m\frac{g}{p}x_{c.g.} = 0 \\ & m\ddot{y}_{c.g.} + m\frac{g}{p}y_{c.g.} = 0 \\ & c_4 m\ddot{x}_{c.g.} + c_7 m\ddot{y}_{c.g.} + I_{33}\ddot{\phi} \\ & \qquad + m\left[\left(2c_{10} - \frac{c_4^2}{p} - \frac{c_7^2}{p}\right)\phi + \frac{c_4}{p}x_{c.g.} + \frac{c_7}{p}y_{c.g.}\right] = 0 \end{aligned} \tag{E-15}$$

Which reduce to

$$\begin{aligned} & \ddot{x}_{c.g.} + \frac{g}{p}x_{c.g.} = 0 \\ & \ddot{y}_{c.g.} - \frac{g}{p}y_{c.g.} = 0 \\ & \ddot{\phi} + \frac{mg}{I_{33}p}\left[Y_{c.g.}Y_B + X_{c.g.}X_C + X_{c.g.}\frac{Y_C^2}{X_C} - X_{c.g.}\frac{Y_B Y_C}{X_C}\right. \\ & \qquad \left. - X_{c.g.}^2 - Y_{c.g.}^2\right]\phi = 0 \end{aligned} \tag{E-16}$$

The equations in $x_{c.g.}$ and $y_{c.g.}$ describe the motion of a simple pendulum of length p. The equation in ϕ is also a simple second-order equation completely uncoupled from the two transverse oscillations.

$\phi(t)$ is a sine wave of period

$$T = \left[\frac{I_{33} p}{mg} \cdot c \right]^{1/2} 2\pi \tag{E-17}$$

where c is a function of the system geometry

$$c = \left[Y_{c.g.} Y_B + X_{c.g.} X_C + X_{c.g.} \frac{Y_C^2}{X_C} - X_{c.g.} \frac{Y_B Y_C}{X_C} - X_{c.g.}^2 - Y_{c.g.}^2 \right]^{-1} \tag{E-18}$$

This period is the quantity measured in the moment of inertia procedures.

Nomenclature -

p = lengths of pendulum wires
A, B, C = points fixed in body geometry
ϕ = rotation about body z-axis
θ_1 = rotation about body x-axis
θ_2 = rotation about body y-axis
$\vec{d}_A$ = vector displacement in lab of point a
$\vec{x}, \vec{y}$ = x and y components of that displacement
c_n = constants in system geometry
TE = kinetic coenergy
m = system mass
I_{nm} = components of moment of inertia tensor
v = potential energy
g = acceleration due to gravity (positive down)
t = time
t_1, t_2 = limits of integral
$\dot{}, \ddot{}$ = single and double differentiation with respect to time
$\frac{\partial}{\partial \xi}$ = partial differentiation with respect to ξ
c.g. = center of gravity
T = rotational period

Appendix F

The computer program (Figs. F-1 and F-2) was written for the Univac 1108 computer at the NASA facility in Slidell, Louisiana. No attempt was made at programming or formating elegance.

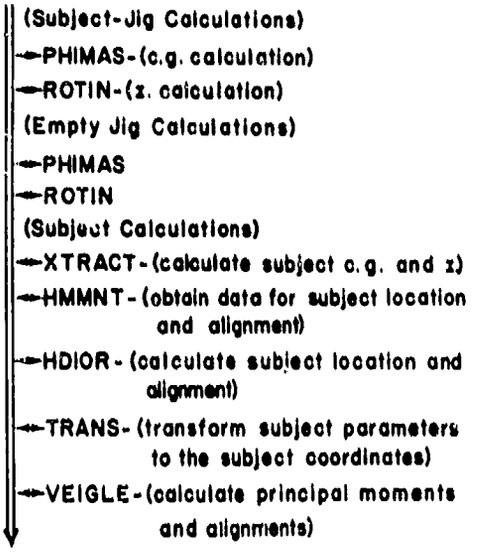

Fig. F-1 · Main program

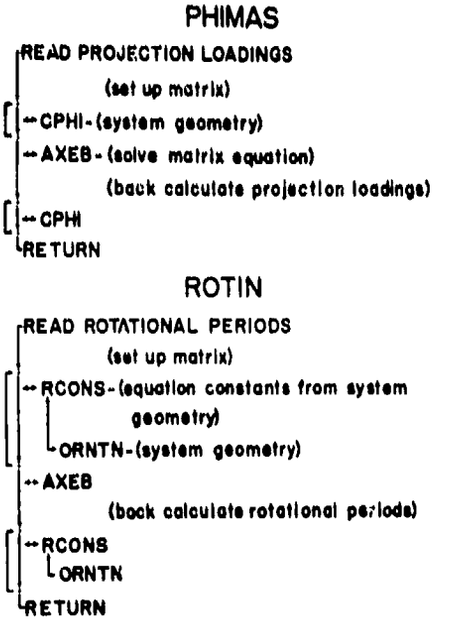

Fig. F-2 · Phimas and rotin programs

Becker, Edward B., "Measurement of Mass Distribution Parameters of Anatomical Segments"

ADDENDUM

MAXIMUM EXPECTED ERROR

In each of the center of gravity measurements, the ratio of the measured projection loading, to the total system weight, yields the position of the system c.g. along a distance X_L. The error in a single measurement ΔW would lead to a location error for the c.g. of:

$$\Delta X_{cg} = \frac{\Delta W}{W_T} X_L$$

Since these c.g. measurements are distributed symmetrically about the jig, the worst case possible arising from comparing the twelve measurements doubles the error. Applying equation 16 leads to an error in the specimen c.g. location of:

$$\Delta X_{cgs} = 4\frac{\Delta W}{W_s} X_L$$

This error is the magnitude of the worst possible vector dislocation of the subject center of gravity and assumes that the vector errors of the two sets of measurements, subject-jig and jig, are worst case and parallel.

Errors in the locations of the jig and subject-jig centers of gravity lead directly to errors in 'C', a function of system geometry occurring in equation 10. The worst case error in 'C' is given by

$$\Delta C = 2C^2 R \frac{\Delta W}{W_J} X_L$$

where R is the distance of the system c.g. from the geometrical center of the system hanging points and whose greatest value is about 5 cm.

The resulting error to the calculated subject moment of inertia is about .5%.

The timing errors in the rotational period measurements are on the order of ten milliseconds. Comparing this to a total measured time of 150 seconds gives a resulting error in the calculated moment of inertia of much less than one percent.

In equation 17, however, the calculated jig and subject-jig centers of gravity are employed to calculate the subject moments of inertia:

From equation 17

$$I_{ii_s} = I_{ii_{sJ}} - I_{ii_J} + \frac{1}{g} \left[W_{sJ} X^2_{KCG\,sJ} - W_s X^2_{KCG\,s} - W_J X^2_{KCG\,J} \right]$$

Let $W_J / W_s = X$

$$I_{ii_s} = I_{ii_{sJ}} - I_{ii_J} - \frac{1}{g} X (X+1) W_s (X_{KCG\,sJ} - X_{KCG\,J})^2$$

Taking the worst case vector errors in the subject-jig and jig c.g. locations as parallel to the line connecting these two points yields the worst case error in I_{ii_s}:

$$\Delta I_{ii_s} \cong \frac{1}{g} 2 \Delta W (2X+1) X_i (X_{KCG\,sJ} - X_{KCG\,J})^2$$

The second largest source of error (the largest arising from the deterioration of the specimens) then, is that arising from the errors in the measurements of the projection loadings.

Taking the accuracy of the projection loadings as .02 pounds, the specimen weight as about 8 pounds, and the ratio of the specimen weight to the jig weight as 3, yields as the worst possible error for the subject c.g.

$$\Delta X_{CG\,s} \cong .64 \text{ cm}$$

and since

$$(X_{KCG\,sJ} - X_{KCG\,J}) < 1.5 \text{ cm}$$

the worst possible error for the subject moment of inertia:

$$\Delta I_{ii_s} \cong .40 - 04 \text{ KG} - \text{M}^2$$

which is less than 4% of any of the principal moments encountered in the specimens.